04

Mechanism of subnanosecond switching in eptron

© P.A. Bokhan[1], P.P. Gugin[1], D.E. Zakrevsky[1,2], V.A. Kim[1], M.A. Lavrukhin[1], I.V. Schweigert[1,3]

[1] Rzhanov Institute of Semiconductor Physics, Siberian Branch, Russian Academy of Sciences, Novosibirsk, Russia
[2] Novosibirsk State Technical University, Novosibirsk, Russia
[3] Khristianovich Institute of Theoretical and Applied Mechanics, Siberian Branch, Russian Academy of Sciences, Novosibirsk, Russia
E-mail: zakrdm@isp.nsc.ru

Received December 26, 2024
Revised March 18, 2025
Accepted March 24, 2025

The initial stage of breakdown in an eptron — a device based on capillary discharge and plasma cathode — has been studied. It is shown that in the general case the discharge develops in two stages due to different mechanisms of plasma generation in the capillary and cathode, which leads to reflection of ionization wave from weakly ionized plasma of the cathode. Artificial increase of its concentration brings both stages closer together and allows obtaining subnanosecond switching times.

Keywords: breakdown, switching, nanoseconds, current development rate.

DOI: 10.61011/TPL.2025.06.61300.20238

The construction of plasma high-voltage switching devices based on the self-breakdown of a combination of a capillary discharge and a plasma cathode (eptrons) [1–3] opens up new possibilities in certain power electronics applications. Of particular note are the pumping and enhancement of frequency-energy parameters of atom and ion self-terminating lasers [2,4,5], the excitation of a volume atmospheric-pressure gas discharge without preliminary ionization [3,6,7], etc. (see, e.g., [8]). These applications are made possible by the capacity of an eptron to operate at voltages up to hundred of kilovolts and pulse repetition rates of tens to hundreds of kilohertz with nano- and subnanosecond excitation pulse fronts [2].

One of the features of an eptron, which has been revealed in the very first studies [1] and has a negative influence on its performance, is that the breakdown in it proceeds in two stages. Although the leading-edge time of a voltage pulse at the active load was often shorter than 1 ns, the overall current settling time exceeded several nanoseconds, which reduced the switching efficiency to $\sim 80-90\,\%$ at this stage and was accompanied by oscillations of both the voltage pulse at the load and the current through it. This stimulates further detailed research into the initial stage of breakdown with nanosecond temporal resolutions, which was exactly the goal of the present study.

A theoretical and experimental investigation of the initial stage of breakdown in a discharge device consisting of a capillary section with a plasma cathode was conducted for this purpose. A numerical study of the discharge ignition dynamics was carried out in a discharge cell with a geometry (Fig. 1) identical to the experimental one. Hydrodynamic and kinetic methods were used in modeling. The system of equations characterizing the discharge dynamics included the Boltzmann equation for the fast electron distribution function; the continuity equation for electrons, ions, atoms, and the average electron energy; and the Poisson equation for the distribution of the potential and the electric field strength. Since the energy of fast electrons emitted from the cathode is not a local function of the electric field strength, their dynamics was modeled by the *ab initio* particle-in-cell method with Monte Carlo collision simulations. The initial plasma concentration was calculated based on the results of modeling the plasma decay in the post-pulse period over $10-50\,\mu$s, which corresponds to pulse repetition rate $f = 100-20\,$kHz.

It turned out that an ionization front forms at the anode surface with an increase in voltage U in a wide range of process parameters. This front starts to move along the dielectric channel with a velocity that depends on operating voltage U. At $U \geqslant 12\,$kV, its velocity exceeds $\sim 10^7\,$cm/s. Figures $1, a, b$ show the example calculated distributions of the potential and the electron concentration at a point in the process of propagation of an ionization wave along the dielectric channel when it has not yet reached the cathode. Numerical modeling of breakdown in a capillary was carried out within the hydrodynamic approximation for the experimental conditions. It is evident from Fig. $1, b$ that a potential well is formed at the boundary of the transition from the capillary to the cathode cavity. This well isolates quasi-neutral plasma of the cathode from the capillary, which translates into reflection of the ionization wave and the emergence of oscillations. Further evolution of the discharge is supported by secondary processes of electron emission from the cathode.

Two eptron designs (inset in Fig. $2, a$) with operating voltage U up to 50 kV, the same capillary structure, and different plasma cathodes were used for the experimental study of the initial stage of breakdown. The capillary structure 50 mm in

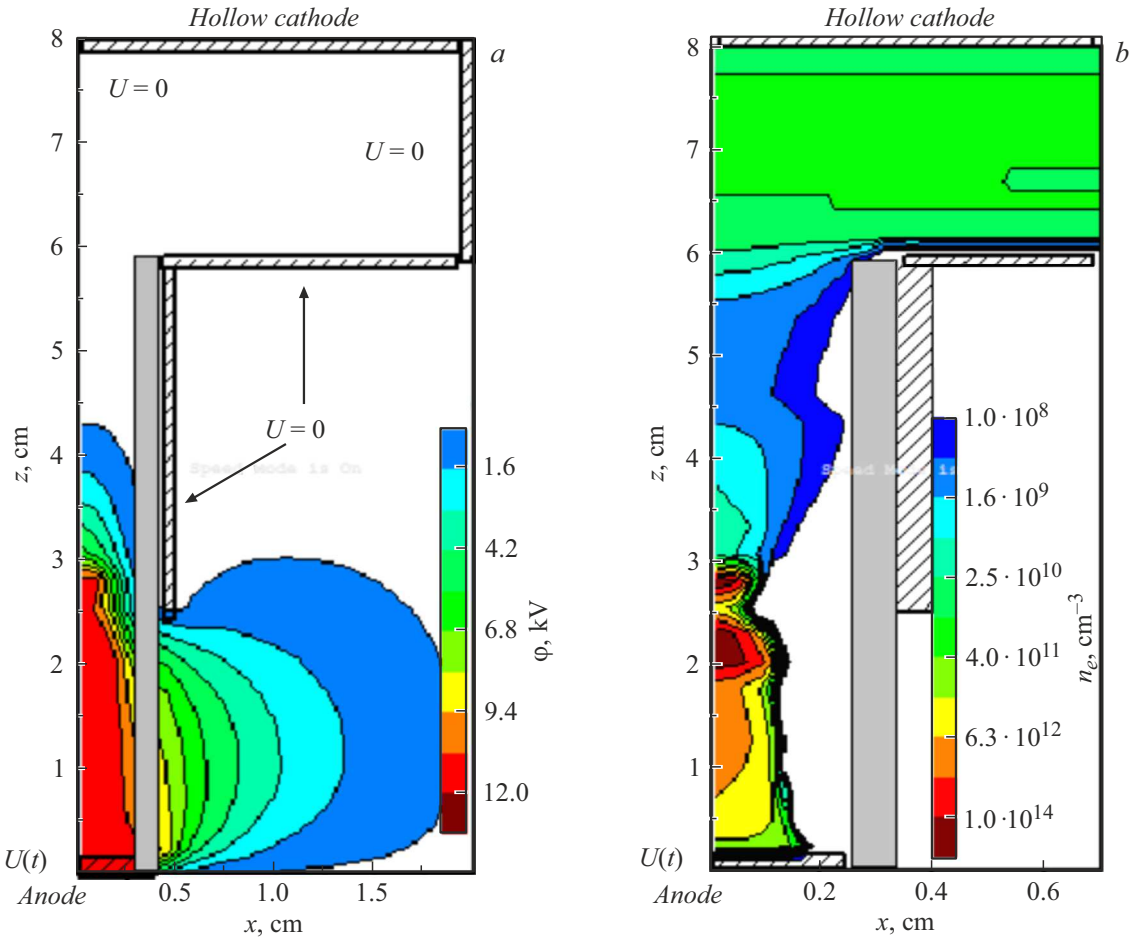

Figure 1. Distributions of the potential (a) and the concentration of electrons (b). $p_{\mathrm{He}} = 4$ Torr.

length with a cross-section of 1×15 mm was a dielectric Al_2O_3 ceramic channel of the rectangular meander type with a pitch of 6 mm: spike (1 mm) + groove (5 mm). In the first case, a discharge in a cylindrical hollow cathode made of silicon carbide (SiC) with internal diameter $d = 28$ mm and length $l = 24$ mm (a volume of 15 cm^3) was used to form the plasma cathode. In the second case, a stainless steel cathode with $d = 13$ mm and $l = 11$ mm (a volume of 1.5 cm^3) was used. This reduction of volume of the hollow cathode made it possible to produce plasma with a higher density. Anode input was arranged on the other side of the cathodes to establish an ignition discharge. Its parameters were the same for both cathodes and were achieved in the discharge of capacitance $C_1 = 500$ pF, which was charged to voltage $U = 5$ kV, through a resistance that could be adjusted within the range of 0–300 Ω. This allowed us to produce plasma with an estimated electron concentration up to $n_e \approx 5 \cdot 10^{13}$ and $5 \cdot 10^{14}$ cm^{-3} in eptrons with SiC and stainless steel cathodes, respectively. Experiments were carried out in He, Ne, H_2, and mixtures of He(Ne) with H_2 under excitation by a train of 20 pulses (train repetition rate, 25 Hz; pulse repetition rate in a train, up to $f = 100$ kHz). Quasi-stationary characteristics were established by the 2nd (3rd) pulse, and all measurements were carried out for the 13th pulse. The main working capacitance had the same value: $C_2 = 500$ pF. Signals were recorded using a Tektronix MDO3104 oscilloscope with a bandwidth of 1 GHz and a sample rate of 5 GHz.

Similar switching characteristics were observed in all the examined cases. For example, the breakdown for the SiC cathode at hydrogen pressure $p_{H_2} = 1$ Torr, $f = 15$ kHz, and $U = 15$ kV without an ignition discharge features two stages with voltage rise times of 1 and 1.5 ns. Owing to a shift between them, the total current settling time is $\tau \approx 7$ ns. With the introduction of an ignition discharge, this time decreases to $\tau \sim 3$ ns. In contrast to the mode without ignition, the major part of voltage at the load (up to ~ 70 %) is applied at the first stage. With an increase in pulse repetition rate to $f > 15$ kHz, the stages are brought closer together; at $f > 50$ kHz, they merge into a single pulse. The leading-edge time at $f > 70$ kHz is $\tau \sim 1.7$ ns. An increase in pressure and operating voltage makes both the interval between the stages and the switching time shorter.

The discharge with a short-circuited load was examined in order to determine the nature of two stages of current evolution. Figure 2, a shows the oscilloscope records of

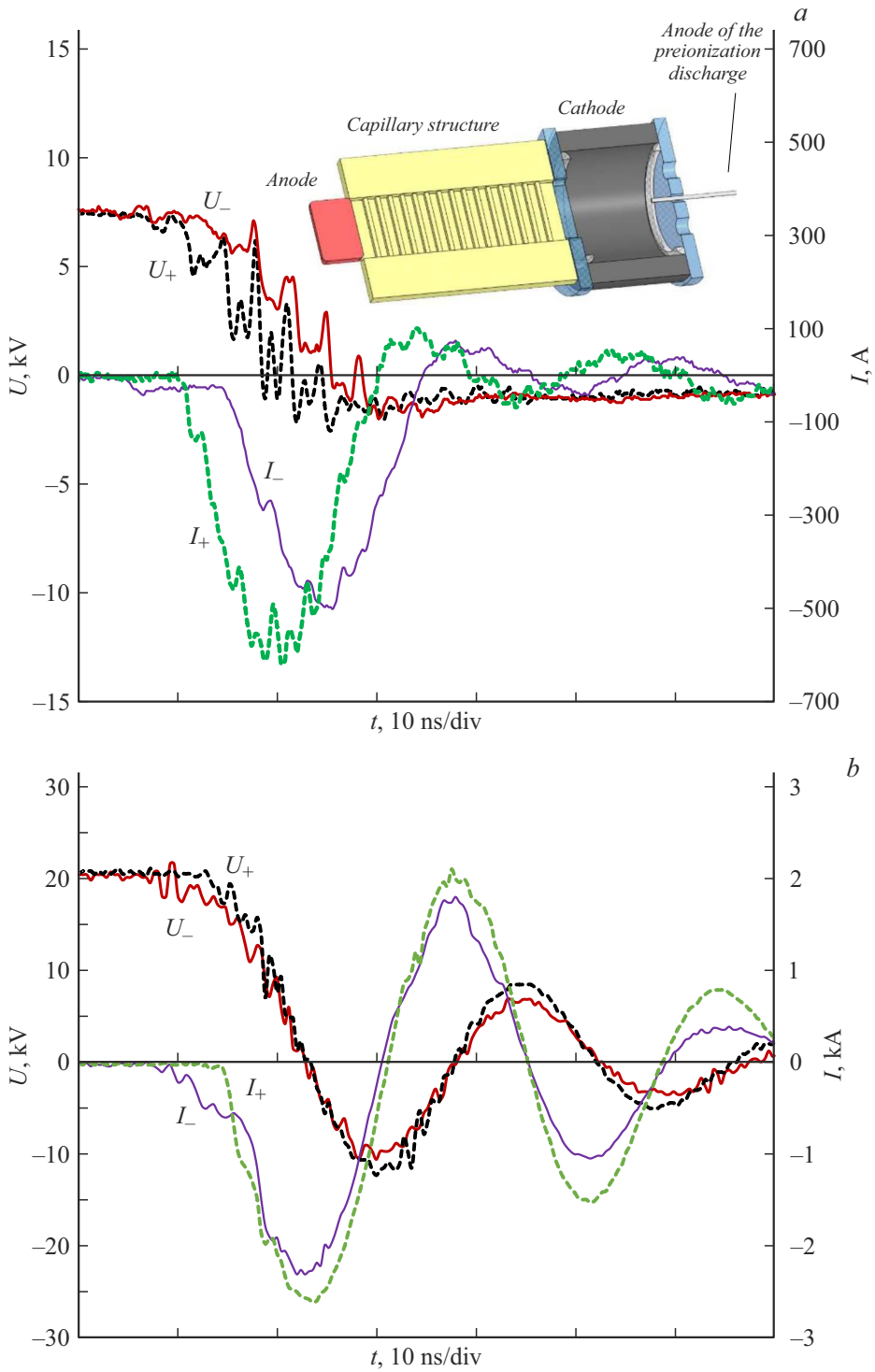

Figure 2. Oscilloscope records of voltage and current with (U_+, I_+) and without (U_-, I_-) an ignition discharge, $R = 0.1\,\Omega$. *a* — cell with a SiC cathode (H_2, $p_{H_2} = 2$ Torr, $f = 2.5$ kHz); *b* — cell with a stainless steel cathode (He, $p_{He} = 6$ Torr, $f = 10$ kHz).

voltage at the eptron anode and the current through it at $U \approx 7.5$ kV for a discharge in hydrogen with $p_{H_2} = 2$ Torr without and with an ignition discharge in the cell with the SiC cathode. It is clearly visible that a „low-current“ discharge with a duration of ~ 10 ns is ignited first and then turns into a „high-current“ one. With increasing voltage, the „low-current“ stage becomes shorter; at $U = 18.5$ kV, its duration is ~ 4 ns. When an ignition discharge is introduced, the stages merge, but the rate of current rise in the first 2–3 ns is twice as low as in the next 3–4 ns. Spikes with a duration of ~ 0.5 ns (Fig. 2, *a*), which arise due to the reflection of the ionization wave from the cathode

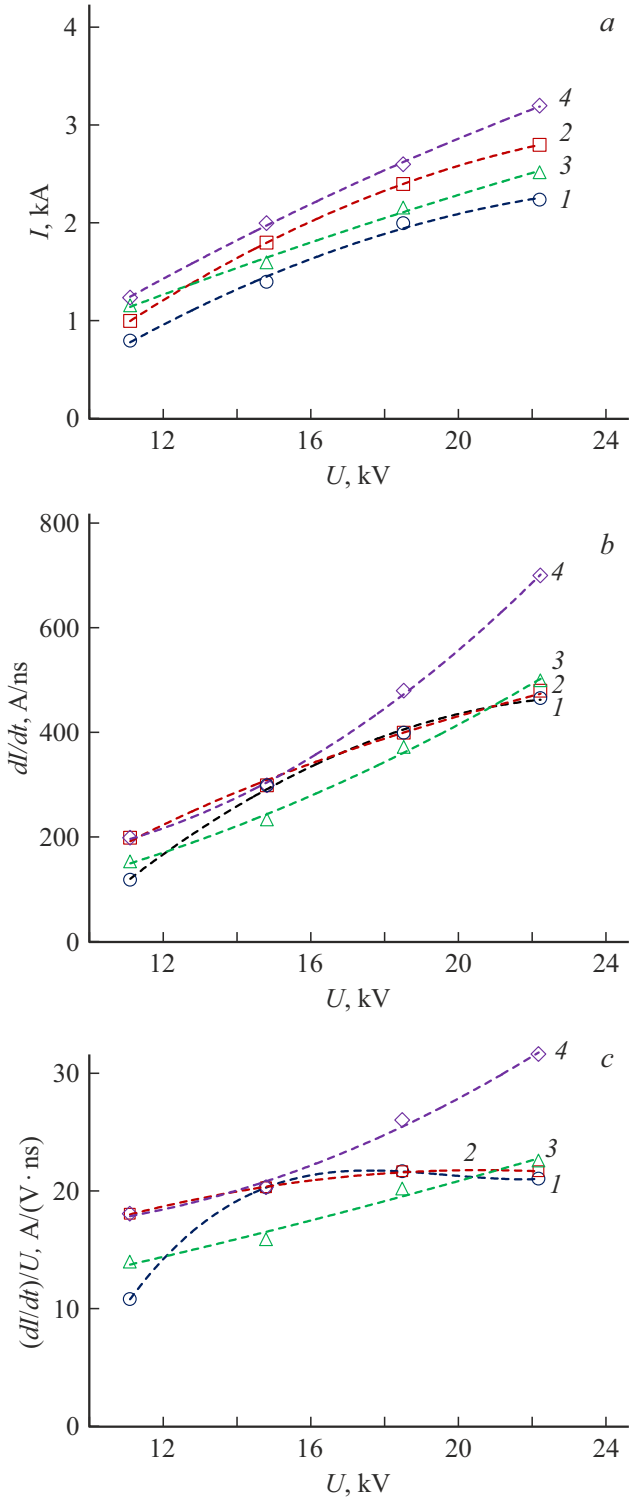

Figure 3. Dependences of current I (a), rate of current rise dI/dt (b), and parameter $(dI/dt)/U$ (c) on voltage U. *1* — He ($p_{He} = 6$ Torr), *2* — Ne ($p_{Ne} = 3$ Torr), *3* — H_2 ($p_{H_2} = 3$ Torr), *4* — He+H_2 ($p_\Sigma = p_{He} + p_{H_2} = 4 + 2 = 6$ Torr).

cavity, are seen in all cases in the oscilloscope records of U and I. The oscillation amplitude and the interval between the breakdown stages decrease with an increase in working

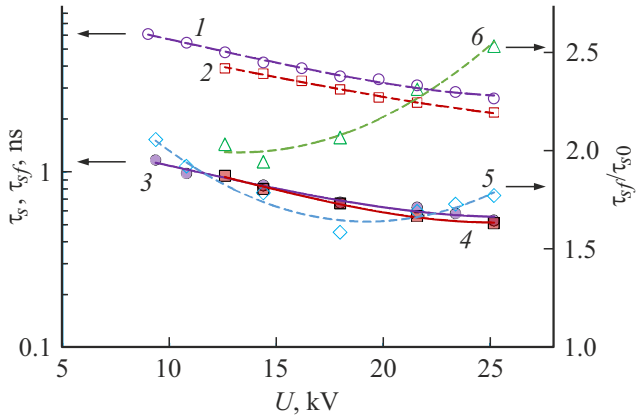

Figure 4. Voltage U dependences ($f = 30$ kHz) of switching time without an ignition discharge τ_s (*1*, *2*), switching time with an ignition discharge τ_{sf} (*3*, *4*), and parameter τ_{sf}/τ_{s0} (*5*, *6*). *1*, *3*, *5* — H_2, $p_{H_2} = 3$ Torr; *2*, *4*, *6* — He+H_2, $p_\Sigma = p_{He} + p_{H_2} = 4 + 2 = 6$ Torr.

gas pressure, anode voltage, pulse repetition rate, and initial electron density in the cathode cavity; in the cell with the stainless steel cathode, they become indistinguishable (Fig. 2, b), and current rise rate dI/dt exceeds hundreds of amperes per nanosecond. Figures 3, a–c present the dependences of amplitude I of current through the eptron, its rise rate dI/dt, and parameter $(dI/dt)/U$ on voltage U under various pressure conditions for different gases in the eptron with the stainless steel cathode. It follows from these data that the rate of current rise increases faster than the initial voltage; i.e., the inductance in the discharge circuit does not yet restrict the current rise rate, and the obtained value of $dI/dt \approx 700$ A/ns is not the limit for the studied eptron design.

When the specified dI/dt are achieved, switching time τ_s does not become equal to ratio $I/(dI/dt)$, since the eptron voltage decreases in the process of switching. Figure 4 shows the dependences of τ_s on initial voltage U at the eptron with H_2 ($p_{H_2} = 3$ Torr) and the $He + H_2$ mixture ($p_\Sigma = p_{He} + p_{H_2} = 4 + 2 = 6$ Torr) at load resistance $R = 80\,\Omega$. It is evident that switching time τ_{sf} with an ignition discharge is several times shorter than without it. In turn, the experimentally measured time τ_s is 1.5–2 times greater than the time calculated as $\tau_{s0} = I/(dI/dt)$. This is attributable, on the one hand, to a voltage reduction in the process of switching and, on the other hand, to the fact that the oscilloscope bandwidth is insufficient. This is the reason why the value of τ_{sf}/τ_{s0} increases for the $He + H_2$ mixture at $U > 15$ kV. The switching efficiency is the highest (exceeds 95 %) in the case when the ignition pulse ends $\Delta t = 0$–50 ns before the capillary breakdown. The energy spent on plasma production in the cathode does not exceed a few percent of the energy dissipated at the load at $U > 20$ kV.

The data presented above suggest that the two-stage nature of switching in the eptron is attributable to the

difference in mechanisms for plasma production in the capillary and the cathode cavity, which leads to reflection of the ionization wave and the emergence of current and voltage oscillations at the breakdown stage. If the charge concentration in the cathode plasma is raised artificially by increasing either the pulse repetition rate or the specific energy input of the ignition pulse, the two-stage nature of breakdown is rectified, and its duration decreases to subnanosecond levels.

Funding

This study was supported financially by the Russian Science Foundation, grant No. № 24-19-00037 (https://rscf.ru/project/24-19-00037/).

Conflict of interest

The authors declare that they have no conflict of interest.

References

[1] P.A. Bokhan, P.P Gugin, M.A. Lavrukhin, D.E. Zakrevsky, J. Phys. D, **51**, 364001 (2018). DOI: 10.1088/1361-6463/aad351
[2] P.A. Bokhan, E.V. Belskaya, P.P. Gugin, M.A. Lavrukhin, D.E. Zakrevsky, I.V. Schweigert, Plasma Sources Sci. Technol., **29**, 084001 (2020). DOI: 10.1088/1361-6595/ab9d91
[3] P.A. Bokhan, P.P. Gugin, D.E. Zakrevsky, M.A. Lavrukhin, Tech. Phys. Lett., **50** (10), 5 (2024). DOI: 10.61011/TPL.2024.10.59684.19992.
[4] M.A. Lavrukhin, P.A. Bokhan, P.P. Gugin, D.E. Zakrevsky, Opt. Laser Technol., **149**, 107625 (2022). DOI: 10.1016/j.optlastec.2021.107625; ibid. **170**, 110174 (2024). DOI: 10.1016/j.optlastec.2023.110174
[5] A.A. Yurkin, Quantum Electron., **46**, 201 (2016). DOI: 10.1070/QEL15754.
[6] [A.A. Yurkin, Instrum. Exp. Tech., **65** (5), 755 (2022). DOI: 10.1134/s0020441222050104.
[7] R. Brandenburg, Plasma Sources Sci. Technol., **26**, 053001 (2017). DOI: 10.1088/1361-6595/aa6426
[8] *Pulsed discharge plasmas. Characteristics and applications*, ed. by T. Chao, Ch. Zhang (Springer, 2023). DOI: 10.1007/978-981-99-1141-7

Translated by D.Safin